International Journal of Applied Pharmaceutics

ISSN- 0975-7058 Vol 14, Issue 2, 2022

Original Article

GREEN SYNTHESIS OF NANOSTRUCTURED ZINC PARTICLES USING AQUEOUS LEAF EXTRACT OF *SCHREBERA SWIETENIOIDES* ROXB. AND THEIR CATALYTIC APPLICATION IN DEGRADATION OF METHYL ORANGE, CRYSTAL VIOLET DYES AND CHROMIUM METAL

S. LAKSHMI TULASI[1], A. V. V. S. SWAMY[2*], P. PAVANI[3], V. SUBHASHINI[4]

[1,3]Department of Freshman Engineering PVP Siddhartha Institute of Technology, Kanuru, Vijayawada, India, [2,4*]Department of Environmental Science, Acharya Nagarjuna University, Guntur, India
Email: arzavvsswamy1962@gmail.com

Received: 26 Nov 2021, Revised and Accepted: 13 Jan 2022

ABSTRACT

Objective: The present work was aimed to synthesized the zinc nanoparticles (ZnO NPs) using aqueous leaf extract of *Schrebera swietenioides* Roxb., and further, the green-synthesized ZnO NPs were studied for its efficacy in the degradation of hazardous dyes like methyl orange, crystal violet and hazardous metal such as chromium.

Methods: The ZnO NPs were synthesized using aqueous leaf extract of *S. swietenioides* Roxb., as a green reducing agent and 0.1 M Zinc acetate as metal source and the NPs synthesis was completed within a short period of 6 h. The ZnO NPs synthesized were characterized using SEM, TEM, EDS, XRD, FT-IR and UV-visible spectrophotometer. Further, the synthesized NPs were applied for reduction of pollutant days such as methyl orange, crystal violet and pollutant metal chromium.

Results: The synthesis of NPs was monitored by observing the color change in the reaction mixture and UV visible spectral analysis. The UV spectral analysis shows a characteristic absorption wavelength at 379 nm. The synthesized NPs were hexagonal wurtzite form crystals having a spherical shape with rough surfaces with an average size of 68 nm and having 73.7 % of zinc content. At a NPs dose of 1.0 g/l the photocatalytic reduction was observed as 85.33±0.02 %, 86.82±0.095 % and 86.73±0.104 % for crystal violet dye, methyl orange dye and chromium metal, respectively. The NPs shows a high % photocatalytic reduction of chromium metal, crystal violet dye and methyl orange dye with less contact time confirms that the synthesized ZnO NPs were effectively catalyzed the degradation of methyl orange, crystal violet dyes and chromium metal. The NPs were observed to be recyclable and can shows high reduction activity after the completion of three cycles of degradation.

Conclusion: Hence it can be concluded that synthesized greener nanocatalyst was efficient for pollutant treatment and demonstrated the power of green biosynthesis for metallic nanoparticles.

Keywords: Zinc oxide nanoparticles, Characterization, TEM, Catalytic application, Methyl orange, Crystal violet, Chromium metal degradation

DOI: https://dx.doi.org/10.22159/ijap.2022v14i2.43697. Journal homepage: https://innovareacademics.in/journals/index.php/ijap

INTRODUCTION

Nanoparticles have gained immense importance in recent times due to their diverse application in the field of science and technology. By definition, they are described as microscopic particles that have size smaller than 100 nm in at least one dimension [1]. Their microscopic size, morphology and distribution enable them to possess unique biological, chemical and physical properties that were distinctly different from those of individual atoms and molecules. Metal nanoparticles have been extensively explored due to their diverse applications in the areas of catalysis, biosensing, medicine, drug delivery etc. [2, 3].

In this advanced and populated era, more comfort and ease of life have increased industrial zones and the rate of production is increased day by day because of the peoples' needs. For the need of wearing clothing and fashion changes, different types of textile industries, including dying, finishing, leather and weaving industries were using different types of chemicals and dyes for production [4]. Among the dyes that are used in various industries, few dyes namely Methyl orange, Methyl red, and Congo Red etc were the most common because of their ease of application and basic colors [5]. Due to the rapid growth in population and industrialization, increased quantities of toxic pollutants such as heavy metals and synthetic organic matters are being released into the aquatic system. Among these toxicants, chromium is one of the most toxic pollutants [6, 7].

The Presence of dyes and metals in water would be very harmful to the aquatic environment as well as humans. Efficient dye and metals degradation has become a challenging task for environmental engineers as well as scientists. Different methods have been adopted by scientists for the degradation of dyes in effluent, which includes biological degradation, photocatalysis and adsorption tactics, etc [8]. But these processes are not sufficient for the removal of pollutants as the load is very high. So, there is a need to search for more advanced techniques to handle these types of pollutants.

ZnO nanoparticles (ZnO NPs) have drawn the attention of several researchers for their exclusive optical and chemical behaviors, which are strongly related to their nano size and morphology [9, 10]. Within the large family of metal oxide nanoparticles, ZnO NPs have impressive properties, including large binding energy, wide band gap, and high piezoelectric features [11]. ZnO NPs have a highly promising prospective in biological functions such as drug delivery and nanomedicine [12], gene delivery [13], along with antibacterial [14], anti-biofilm [15], antifungal [16], larvicidal and anti-diabetic activities [17]. In view of the above, the present work intended to synthesis the Zinc oxide (ZnO) NPs using aqueous leaf extract of *Schrebera swietenioides* Roxb. Further, the synthesized NPs were studied for its effectiveness for the removal of pollutant dyes such as methyl orange and crystal violet. Further, the reduction of pollutant metal Chromium using synthesized ZnO NPs was evaluated.

MATERIALS AND METHODS

Collection of plant material

The leaves of *S. swietenioides* plant were collected in Tirumala hills, Tirupati. The plant material was identified by Dr. Ch. Srinivasa Reddy, Assistant Professor, Department of Botany, SRR and CVR Government Degree College (A) Vijayawada and a dried specimen was stored in the department with specimen number SRR-CVR/2019-20/Bot/31. The fresh leaves were shade dried, powdered and the powdered plant material was used for the synthesis of NPs.

Chemicals and reagents

The chemicals used the study, such as Zinc acetate, sodium hydroxide, potassium dichromate, methylene blue, methyl orange, diphenyl carbazide etc were the reagent grade chemicals and were purchased from Merck chemicals, Mumbai.

Preparation of aqueous leaf extract

An accurately weighed 1 gram of the dried leaf powder was taken in a beaker containing 100 ml of water. Heat the content on a magnetic stirrer at 70 °C for 1 H. Then it was cooled and filtered using Whatman filter paper.

Green synthesis of zinc oxide nanoparticles

The solution 1 for the synthesis of NPs was prepared by stirring 9:1 (v/v) aqueous leaf extract of *S. swietenioides* and Zinc acetate (0.1 M) solution in a magnetic stirrer for 4 H. Sodium hydroxide solution was prepared in aqueous (0.8 M) ethanol and considered as solution B. The solution A and B were mixed and using a magnetic stirrer for 6 h. Then the zinc hydroxide peracetate formed at the bottom of the beaker was collected using centrifugation. Then the obtained particles were heated at 300 °C temperature for 45 min to evaporate the solvent in muffle furnace and to convert zinc hydroxide into ZnO NPs particle powder [18].

Characterization of nanoparticles

The ZnO NPs were characterized for its optical characteristics (UV-visible spectrophotometer; JASCO, Japan), shape (Field emission scanning electron microscope-NOVA NANOSEM 450, FEI, USA), crystal nature (x-ray diffractometer; Rigaku Corporation, Japan), elemental composition (RONTEC's EDX system; QuanTax 200, Germany), topography (Transmission Electron Microscope; Jeol/JEM 2100, Japan) and the bioactive functional groups responsible for the formation of NPs (FT-IR spectrophotometer; Bruker, USA).

Photocatalytic experiment

The photocatalytic activity was evaluated by monitoring the degradation of the organic dyes (methyl orange, crystal violet) and chromium metal under visible light irradiation. The catalyst at selected fixed weight was dispersed in 50 ml of the aqueous dye solution at a concentration of 10 ppm of crystal violet, 50 ppm of methyl orange and aqueous metal solution at a concentration of 50 µg/ml separately. The reaction mixture was stirred to get homogenous mixture and then stirring continued in dark for 45 min to attain adsorption-desorption equilibrium. The reaction mixture was exposed to visible light irradiation (70 W mercury lamp) and then an aliquot was taken at 15 min intervals for 2 h. The solution was centrifuged, and the adsorption efficiency was monitored directly at 584 nm for crystal violet, 467 nm for methyl orange and diphenyl carbazide method at 540 nm for chromium metal using UV-Visible spectrometer [19, 20]. The metal and dye adsorption capacity of NPs was calculated using the equations.

$$\text{Adsorption capacity} = \frac{\text{initial concentration} - \text{concentration at a specific time}}{\text{weight of the adsorbent}} \text{X volume of dye} \quad \ldots (1)$$

Recyclability and photostability of ZnO NPs

The recyclability of catalytic activity of the synthesized ZnO NPs was evaluated by repeating the catalytic activity as per the procedure described above. Each study cycle, the catalyst (ZnO NPs) was washed 3 times with distilled water using a magnetic stirrer to remove the dye completely from the particles. Then they are dried using vacuum 40 °C for 6hours. The dried particle was used for a further cycle of catalytic activity [21].

RESULTS

The UV–visible absorption spectra (fig. 1A) give the primary information for the formation of NPs and shows the characteristic sharpened nature of the absorption peak at a wavelength of 379 nm proves that the NPs were mono-dispersed with narrow size distribution of particles [22]. The type of bioactive molecules or functional groups that are actively involved to bind the metal and formation of NPs was evaluated by shifting in wavenumber in FT-IR spectrum. The FT-IR spectral analysis (fig. 1B) confirms the presence of various bioactive functional groups in the NPs such as free-OH in alcohols (3668 cm^{-1}), intramolecular bonded alcohols (3461 cm^{-1}), N-H stretching in amine salts (2800-3000 cm^{-1}), C-H stretching in alkanes (3005 cm^{-1}), C-N stretching in aromatic amines (1314 cm^{-1}) and aromatic esters (1287 cm^{-1}). These functional group corresponding to bioactive compounds that are actively involved in the formation of NPs. The SEM analysis (fig. 1C) confirms that the NPs were spherical shape with rough surfaces. The Zn metal composition of 73.7 % with Zn was identified at 8.61 (Kα) and 1.09 keV (Lα) in EDS analysis data (fig. 1D). It was also confirmed that Oxygen was observed at 0.5 keV, which is another key element in the formation of ZnO NPs. The shape of the synthesized NPs was further characterized using TEM analysis. The TEM image (fig. 1E) clearly demonstrated that most of the ZnO NPs were various spherical shapes with rough surfaces and the results are in correlation with the results observed in SEM analysis. The XRD analysis spectra (fig. 1F) shows 2θ characteristic peaks corresponding to planes of the crystal lattice structure and the peaks corresponding to the lattice planes were identified at 31.60 (100), 34.22 (002), 36.11 (101), 47.35 (102), 56.45 (110), 62.69 (103), 66.11 (200), 67.84 (112), 68.87 (201), 71.70 (004) and 76.64 (202). The peaks are in a good argument with the hexagonal Wurtzite form of the NPs and were correlates with standard JCPDS Card No. 89-0510. The average size of the NPs was confirmed as 68 nm.

Fig. 2A illustrates the temporal evolution of optical absorption spectra of 10 ppm crystal violet dye aqueous solutions with ZnO NPs photocatalyst. It was observed that the intensity of the absorption peak at 584 nm was decreased with increase in irradiation time of ZnO NPs photocatalyst with the crystal violet. The % reduction of crystal violet was observed to be increased with an increase in time. The % degradation of 26.49±0.199, 37.82±0.170, 76.36±0.03 and 85.33±0.02 % was observed with in contact time of 60 min at a catalyst dose of 0.25, 0.5, 0.75 and 1.0 g/l, respectively, confirms the does dependent activity of the NPs (fig. 2C). More than 50 % dye reduction was observed within 30 min for NPs at a dose of 1 g/l, whereas NPs at 0.75 g/l requires 45 min time to reduce the dye more than 50 %. At maximum time of study i. e after 2 h of degradation study, the % dye reduction was 31.61±0.060, 48.94±0.042, 81.95±0.035 and 94.90±0.031, respectively confirms that the ZnO NPs degrade the pollutant drastically with in less time of 60 min. The FT-IR spectrum of dye treated NPs shows (fig. 2B) additional bonds compared with untreated NPs may be due to the functional groups of crystal violet that adsorbed on the surface of the NPs. The rate constant (k) was determined from the linear plot of ln (A_0/A_t) versus reduction time in minutes (fig. 2D). The degradation reaction follows a pseudo-first-order reaction kinetics with respect to crystal violet. The rate constant (k) was calculated as 2.29×10^{-3}, 5.07×10^{-3}, 1.21×10^{-2} and 2.50×10^{-2} respectively for the crystal violet dye reduction study conducted at a nanocatalyst dosage of 0.25, 0.5, 0.75 and 1.0 g/l, respectively.

The methyl orange dye at a concentration of 50 ppm was selected for the dye reduction study. The reduction of methyl orange dye in the aqueous solution was monitored from time to time using a spectrophotometer at a maximum absorption wavelength of 467 nm (fig. 3A). The absorption spectra show the decline in the concentration of methyl orange dye was observed to be increased with increase in time as well as an increase in the dose of the NPs. At 1 h of the catalytic study, the % degradation was observed to be 41.62±0.040, 48.55±0.052, 75.79±0.156 and 86.82±0.095 % for the nano catalyst dose of 0.25, 0.5, 0.75 and 1.0 g/l, respectively (fig. 3C). The proved that the metal reduction was very effective at initial time of the reduction study and by increase in the time, the dye reduction efficiency was decreased due to the blockage of the active sites in the NPs with the dye. The FT-IR spectrum (fig. 3B) also confirms that the dye molecules adsorbed on the surface of the NPs. The kinetics of the reaction was study by plotting the graph by considering ln (A_0/A_t) on the y-axis and reduction time in minutes on x-axis (fig. 3D) and the plot confirms that the degradation follows the pseudo first-order reaction. The rate constant (k) was calculated and found to be 6.61×10^{-3}, 1.07×10^{-2}, 1.64×10^{-2} and 2.68×10^{-2} respectively for the methyl orange dye reduction study conducted at a nanocatalyst dosage of 0.25, 0.5, 0.75 and 1.0 g/l, respectively. Hence it can be

confirmed that the NPs were very effective for the reduction of methyl orange dye from aqueous solution.

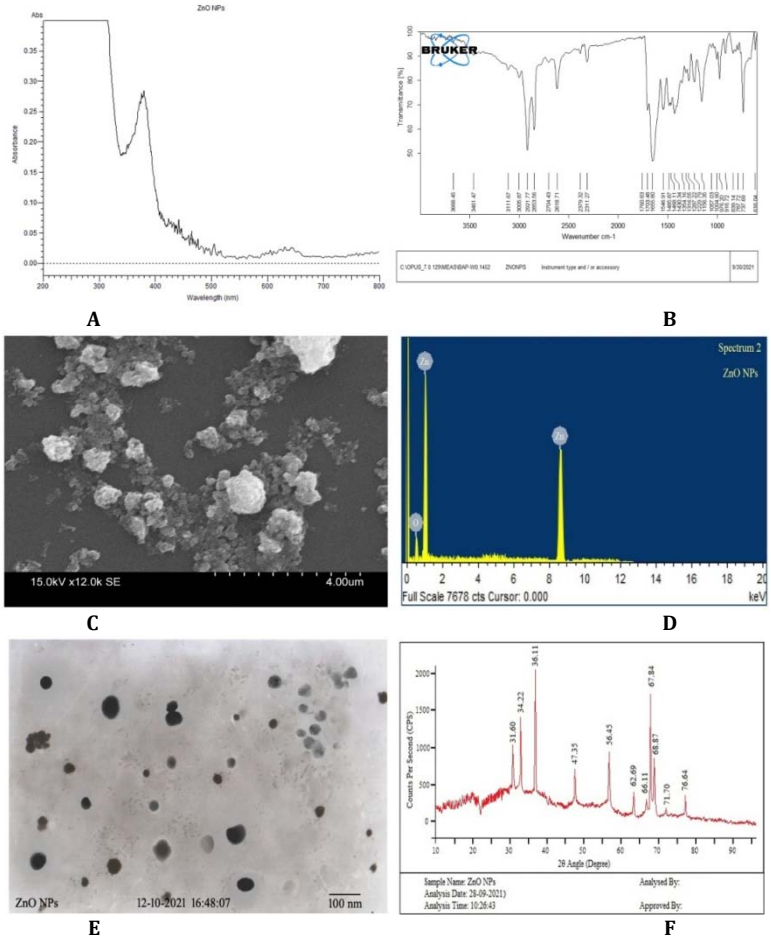

Fig. 1: Characterization of ZnO NPs synthesized using *S. swietenioides* leaf extract, A) UV-visible scanning spectra; B) FT-IR spectra; C) SEM analysis; D) EDS spectra; E) TEM analysis; and F) XRD analysis spectra of the synthesized ZnO NPs

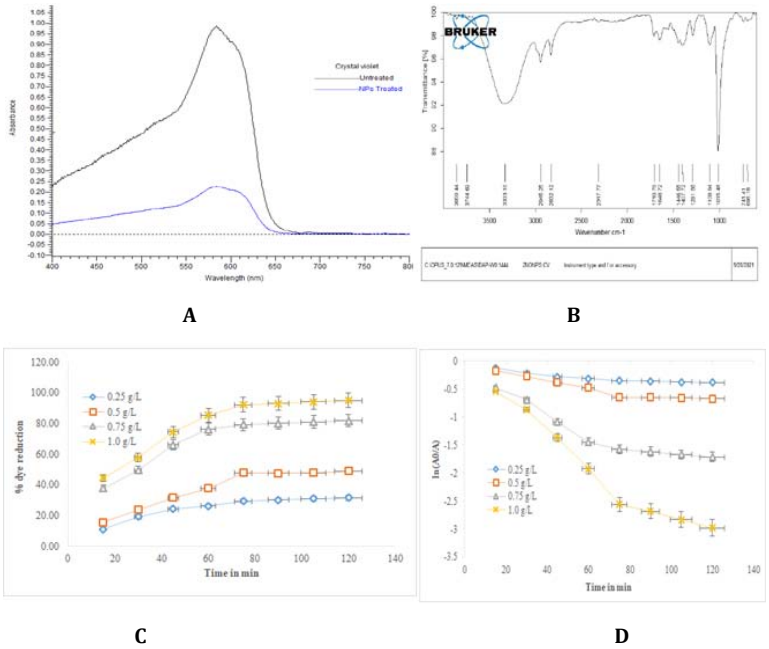

Fig. 2: Photocatalytic degradation of crystal violet dye using ZnO NPs synthesized using *S. swietenioides* leaf extract, the results presented in graphs (C and D) were the mean±SD of three replicate experiments, A) Temporal evolution of the absorption spectra of 10 ppm crystal violet aqueous solution at 0 h and 2 h in the presence of ZnO nanoparticles; B) FT-IR spectrum of crystal violet treated ZnO NPs showing the functional groups corresponds to crystal violet dye; C) The photodegradation time profile with different strengths of ZnO NPs on the

reduction of crystal violet dye at a concentration of 10 ppm; D) The photodegradation time profile of A_t/A_0 for 50 ppm crystal violet dye concentration treated with various strengths of photocatalyst (ZnO NPs)

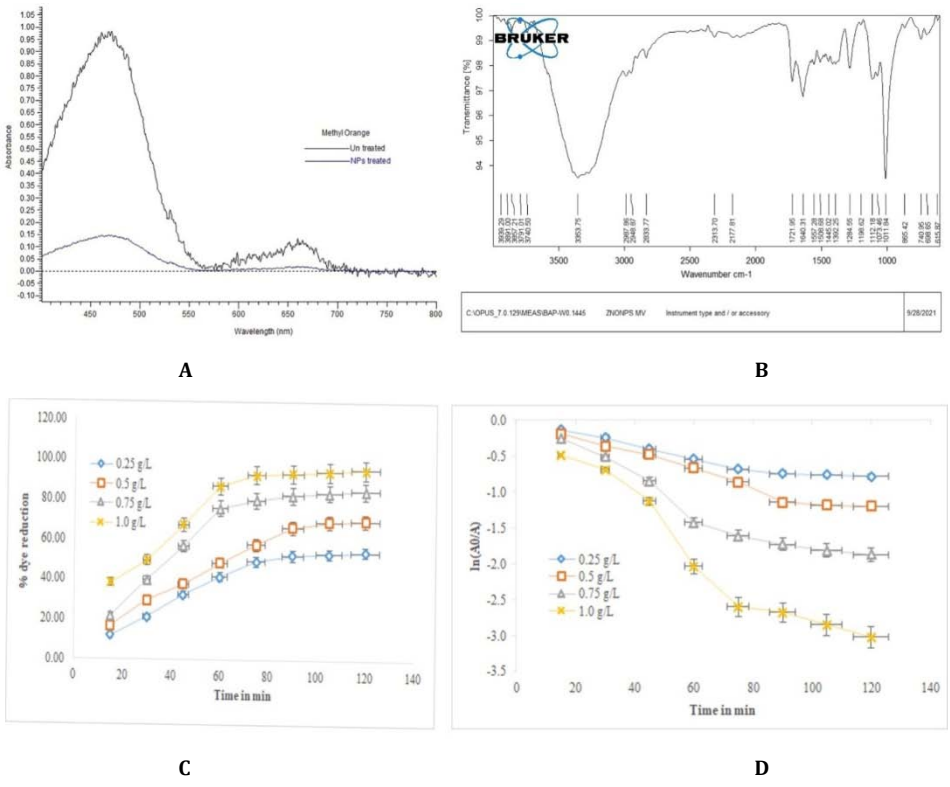

Fig. 3: Photocatalytic degradation of methyl orange dye using ZnO NPs synthesized using *S. swietenioides* leaf extract, the results presented in graphs (C and D) were the mean±SD of three replicate experiments, A) Temporal evolution of the absorption spectra of 50 ppm methyl orange aqueous solution at 0 h and 2 h in the presence of ZnO nanoparticles; B) FT-IR spectrum of methyl orange treated ZnO NPs showing the functional groups corresponds to methyl orange dye; C) The photodegradation time profile with different strengths of ZnO NPs on the reduction of methyl orange dye at a concentration of 50 ppm; D) The photodegradation time profile of A_t/A_0 for 10 ppm methyl orange dye concentration treated with various strengths of photocatalyst (ZnO NPs)

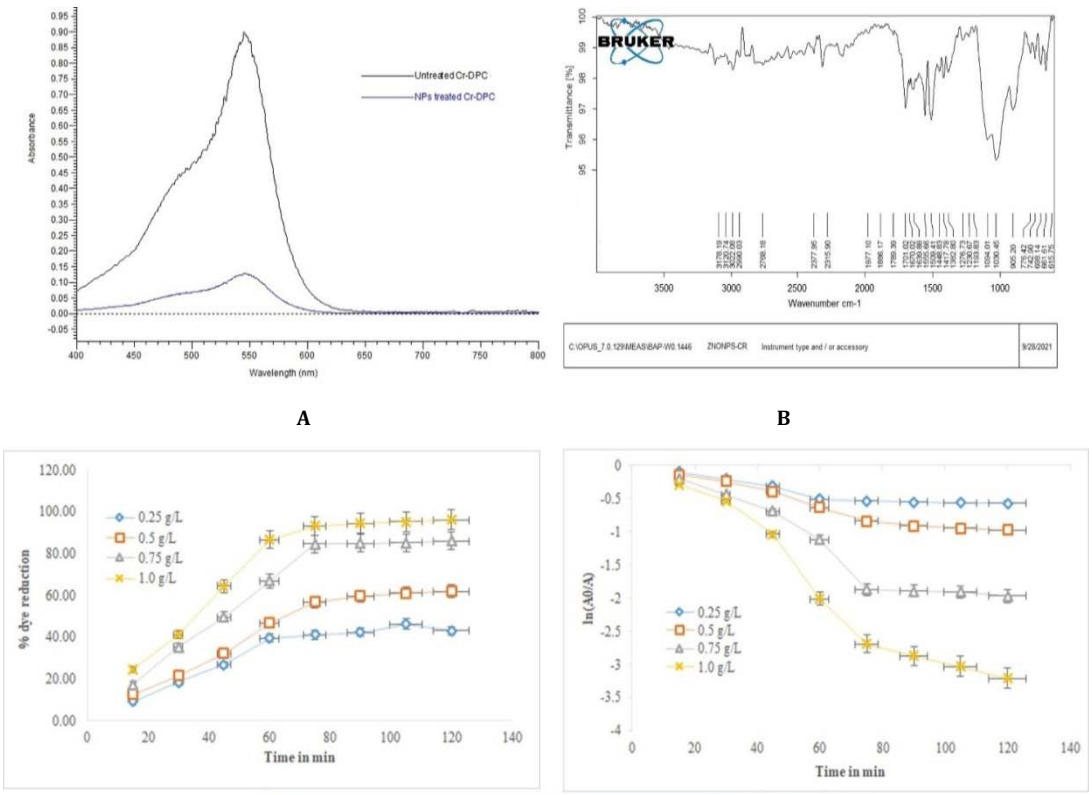

C D

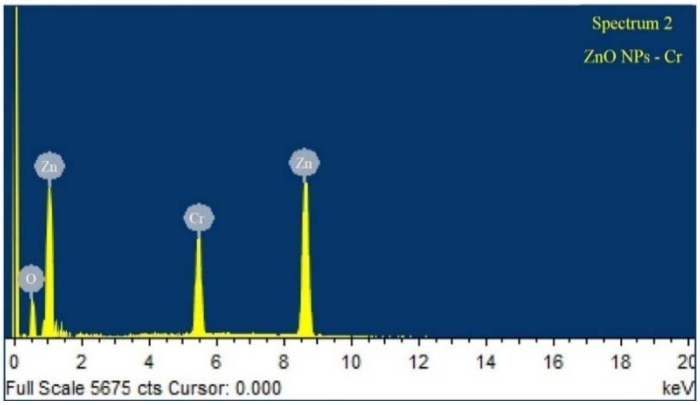

E

Fig. 4: Photocatalytic degradation of methyl orange dye using ZnO NPs synthesized using *S. swietenioides* leaf extract, the results presented in graphs (C and D) were the mean±SD of three replicate experiments, A) Temporal evolution of the absorption spectra of 50 ppm chromium metal solution treated with diphenyl carbazide at 0 h and 2 h in the presence of ZnO nanoparticles; B) FT-IR spectrum of chromium treated ZnO NPs showing the reduced intensity of functional groups due to blockage of chromium metal when compared with untreated ZnO NPs; C) The photodegradation time profile with different strengths of ZnO NPs on the reduction of chromium metal at a concentration of 50 ppm; D) The photodegradation time profile of A_t/A_0 for 50 ppm chromium metal concentration treated with various strengths of photocatalyst (ZnO NPs); E) EDS spectra of chromium metal treated ZnO NPs shows peak corresponds to chromium metal

The diphenyl carbazide (DPC) visible spectrophotometer method was adopted for the determination of chromium (Cr) content in the reduction studies carried using synthesized ZnO NPs. The Cr-DPC complex shows characteristic maximum absorption at a wavelength of 540 nm. The ZnO NPs treated Cr-DPC complex shows very less intensity than the untreated Cr-DPC complex (fig. 4A) confirms that the ZnO NPs treatment decreased the chromium content in the aqueous solution. The % metal reduction was observed as 64.39±0.181 % within 45 min at NPs dose of 1.0 g/l whereas at the same time the % reduction was observed to be 26.92±0.046, 32.13±0.057 and 49.58±0.036 % for NPs at 0.25, 0.5 and 0.75 g/l confirms the dose-dependent activity of the NPs. At a contact time of 1 h, the % reduction of chromium was observed as 86.73±0.104 % for NPs at 1.0 g/l dose confirms that at this dose, the metal reduction activity was completed with in less time of 1 h (fig. 4C). The Ft-IR spectrum shows of the treated NPs shows the decrease in intensity of the functional groups that are detected in untreated NPs may be due the blockage of functional groups with chromium metal (fig. 4B). The rate constant (k) was determined from the linear plot of ln (A_0/A_t) versus reduction time in minutes (fig. 4D). The degradation reaction follows a pseudo-first-order reaction kinetics. The rate constant (k) was calculated as 4.59×10^{-3}, 8.83×10^{-3}, 1.91×10^{-2} and 3.10×10^{-2} respectively for the chromium metal reduction study conducted at a nanocatalyst dosage of 0.25, 0.5, 0.75 and 1.0 g/l, respectively.

The recyclability of the photocatalyst treated with both dyes crystal violet, methyl orange and chromium metal was evaluated in three photocatalysis process. After three cycles of study, the photocatalytic efficiency was observed to be 98.71 %, 98.27 % and 98.06 for methyl orange, crystal violet and chromium metal, respectively (fig. 5). The results confirm that after three cycles of study, there is the negligible decline in the photocatalytic degradation efficiency for both dyes and metal in the study.

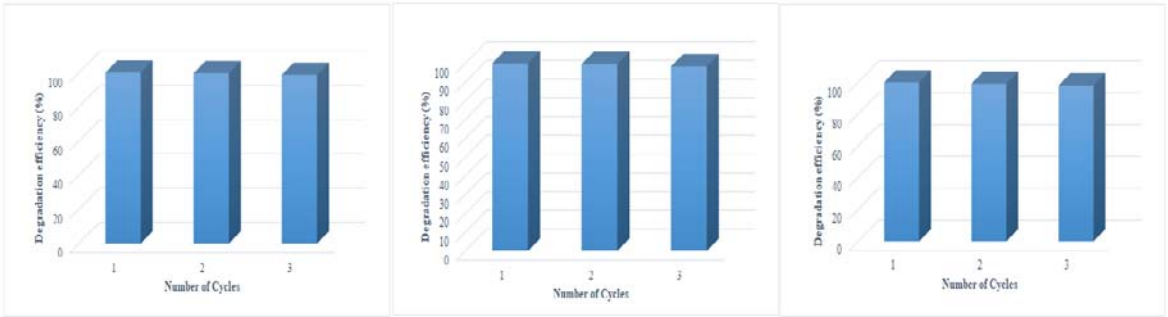

A B C

Fig. 5: Schematic shows the degradation efficiency of ZnO NPs after three cycles, data is expressed as mean, N=3, A) methyl orange; B) crystal violet; C) chromium metal

DISCUSSION

The study aimed to utilize the phytochemical constituents present in the aqueous leaf extract of S *swietenioides* as biological reducing agents for the formation of ZnO NPs. In the initial stage of the synthesis process, the formation of NPs was assessed by the color change in the reaction mixture from light green to dark brown. The NPs were formed by the reaction of Zinc acetate with the phytochemical compounds present in the aqueous leaf extract of S. *swietenioides*. The formed NPs were preserved and further the characterization of NPs and its applications as pollutant adsorbents was evaluated. The preliminary identification of NPs was done by observing characteristic UV-visible absorption maxima at 379 nm, which was in correlation with reported results

[23, 24]. The XRD analysis of synthesized NPs shows characteristic peaks at 31.60 (100), 34.22 (002), 36.11 (101), 47.35 (102), 56.45 (110), 62.69 (103), 66.11 (200), 67.84 (112), 68.87 (201), 71.70 (004) and 76.64 (202) which confirms its hexagonal Wurtzite form of the NPs and were correlate with standard JCPDS Card No. 89-0510. The XRD patter observed in the present study was in good argument with the previous findings [23, 25]. The average size of the NPs was observed to be 68 nm and the % metal content in the synthesized NPs was observed to be 73.7 % which is very higher than the few findings reported [24], which confirms that the metal content was very high in the present study. Hence it can be confirmed that the NPs synthesized in the present study high metal content and significantly less size.

The synthesized ZnO NPs were studied for its efficiency on the reduction of crystal violet dye, methyl orange dye and chromium metal. The NPs were proved to be having efficient dye and metal reduction activity. At a high dose of NPs studied, the photocatalytic efficiency of 94.90±0.031 %, 86.82±0.095 % and 86.73±0.104 % was observed respectively for crystal violet, methyl orange and chromium metal within a very less contact time of less than 2h. The photocatalytic efficient of ZnO NPs reported in the present study was very higher than the many findings reported in the literature [26-28]. Hence it can be confirmed that the NPs synthesized in the study will be the best choice for the photocatalytic degradation of crystal violet, methyl orange dyes and chromium metal.

CONCLUSION

In summary, the biological method for synthesis of ZnO NPs was achieved using aqueous leaf extract of *S. swietenioides*. The method was very fast, simple and eco-friendly due to the non-involvement of harmful chemicals and involvement of active molecules present in aqueous leaf extract of *S. swietenioides*. The synthesized NPs were spherical in shape with rough surfaces, hexagonal wurtzite form crystals with an average size of 68 nm. Based on the EDS elemental analysis, the metal composition was confirmed as 73.7 %. The NPs were applied for the reduction of pollutant dyes crystal violet, methyl orange and metal pollutant chromium. The NPs were proved to be having high photocatalytic activity and were effectively used for the reduction of dyes and metal in the study. Therefore, this study provides an eco-friendly method for the synthesis of ZnO NPs, which can be used in effluent treatment (dye and metal degradation) of different types of industries.

FUNDING

The authors declare that we have “no funding support for this study.”

AUTHORS CONTRIBUTIONS

All authors have contributed equally.

CONFLICT OF INTERESTS

The authors declare that we have no conflict of interest.

REFERENCES

1. Al-Zaban MI, Mahmoud MA, AlHarbi MA. Catalytic degradation of methylene blue using silver nanoparticles synthesized by honey. Saudi J Biol Sci. 2021;28(3):2007-13. doi: 10.1016/j.sjbs.2021.01.003, PMID 33732087.
2. Gupta M. Inorganic nanoparticles: an alternative therapy to combat drug-resistant infections. Int J Pharm Pharm Sci. 2021;13:20-31. doi: 10.22159/ijpps.2021v13i8.42643.
3. Chippa S, Suvarna V. Nanotechnology for detection of diseases caused by viruses-current overview. Int J Pharm Pharm Sci. 2021;13:1-7. doi: 10.22159/ijpps.2021v13i4.40359.
4. Helal SE, Abdelhady HM, Abou Taleb KA, Hassan MG, Amer MM. Lipase from Rhizopus oryzae R1: in-depth characterization, immobilization, and evaluation in biodiesel production. J Genet Eng Biotechnol. 2021;19(1):1. doi: 10.1186/s43141-020-00094-y. PMID 33400043.
5. Wahi RK, Yu WW, Liu Y, Mejia ML, Falkner JC, Nolte W, Colvin VL. Photodegradation of congo red catalyzed by nanosized TiO_2. Journal of Molecular Catalysis A: Chemical. 2005;242(1-2):48-56. doi: 10.1016/j.molcata.2005.07.034.
6. Bianchi V, Zantedeschi A, Montaldi A, Majone F. Trivalent chromium is neither cytotoxic nor mutagenic in permeabilized hamster fibroblasts. Toxicol Lett. 1984;23(1):51-9. doi: 10.1016/0378-4274(84)90009-2, PMID 6485018.
7. Chiu A, Shi XL, Lee WKP, Hill R, Wakeman TP, Katz A, Xu B, Dalal NS, Robertson JD, Chen C, Chiu N, Donehower L. Review of chromium (VI) apoptosis, cell-cycle-arrest, and carcinogenesis. J Environ Sci Health C Environ Carcinog Ecotoxicol Rev. 2010;28(3):188-230. doi: 10.1080/10590501.2010.504980, PMID 20859824.
8. Das R, Sarkar S. Optical properties of silver nano-cubes. Opt Mater. 2015;48:203-8. doi: 10.1016/j.optmat.2015.07.038.
9. Kandula S, Jeevanandam P. Sun-light-driven photocatalytic activity by ZnO/Ag hetero nanostructures synthesized via a facile thermal decomposition approach. RSC Adv. 2015;5(93):76150-9. doi: 10.1039/C5RA14179F.
10. Madhiyazhagan P, Murugan K, Kumar AN, Nataraj T, Subramaniam J, Chandramohan B, Panneerselvam C, Dinesh D, Suresh U, Nicoletti M, Alsalhi MS, Devanesan S, Benelli G. One-pot synthesis of silver nanocrystals using the seaweed gracilaria edulis: biophysical characterization and potential against the filariasis vector culex quinquefasciatus and the midge chironomus circumdatus. J Appl Phycol. 2017;29(1):649-59. doi: 10.1007/s10811-016-0953-x.
11. Fortunato E, Barquinha P, Pimentel A, Gonçalves A, Marques A, Pereira L, Martins R. Recent advances in ZnO transparent thin film transistors. Thin Solid Films. 2005;487(1-2):205-11. doi: 10.1016/j.tsf.2005.01.066.
12. Xiong HM. ZnO nanoparticles applied to bioimaging and drug delivery. Adv Mater. 2013;25(37):5329-35. doi: 10.1002/adma.201301732, PMID 24089351.
13. Nie L, Gao L, Feng P, Zhang J, Fu X, Liu Y, Yan X, Wang T. Three-dimensional functionalized tetrapod-like ZnO nanostructures for plasmid DNA delivery. Small. 2006;2(5):621-5. doi: 10.1002/smll.200500193, PMID 17193097.
14. Applerot G, Lipovsky A, Dror R, Perkas N, Nitzan Y, Lubart R, Gedanken A. Enhanced antibacterial activity of nanocrystalline ZnO due to increased ROS-mediated cell injury. Adv Funct Mater. 2009;19(6):842-52. doi: 10.1002/adfm.200801081.
15. Vijayakumar S, Malaikozhundan B, Shanthi S, Vaseeharan B, Thajuddin N. Control of biofilm-forming clinically important bacteria by green synthesized ZnO nanoparticles and its ecotoxicity on *Ceriodaphnia cornuta*. Microb Pathog. 2017;107:88-97. doi: 10.1016/j.micpath.2017.03.019, PMID 28330748.
16. Sharma D, Rajput J, Kaith BS, Kaur M, Sharma S. Synthesis of ZnO nanoparticles and study of their antibacterial and antifungal properties. Thin Solid Films. 2010;519(3):1224-9. doi: 10.1016/j.tsf.2010.08.073.
17. Alkaladi A, Abdelazim AM, Afifi M. Antidiabetic activity of zinc oxide and silver nanoparticles on streptozotocin-induced diabetic rats. Int J Mol Sci. 2014;15(2):2015-23. doi: 10.3390/ijms15022015, PMID 24477262.
18. Balogun SW, James OO, Sanusi YK, Olayinka OH. Green synthesis and characterization of zinc oxide nanoparticles using bashful (*Mimosa pudica*), leaf extract: a precursor for organic electronics applications. SN Appl Sci. 2020;2(3):504. doi: 10.1007/s42452-020-2127-3.
19. Cavuslar Ozge, Nakay E, Kazakoglu U, Abkenar SK, Ow Yang CW, Acar HY. Synthesis of stable gold nanoparticles using linear polyethyleneimines and catalysis of both anionic and cationic azo dye degradation. Mater Adv. 2020;1(7):2407-17. doi: 10.1039/D0MA00404A.
20. Khoso WA, Haleem N, Baig MA, Jamal Y. Synthesis, characterization and heavy metal removal efficiency of nickel ferrite nanoparticles (NFN’s). Sci Rep. 2021;11(1):3790. doi: 10.1038/s41598-021-83363-1, PMID 33589710.
21. Pant A, Tanwar R, Kaur B, Mandal UK. A magnetically recyclable photocatalyst with commendable dye degradation activity at ambient conditions. Sci Rep. 2018;8(1):14700. doi: 10.1038/s41598-018-32911-3, PMID 30279537.

22. Pai S, HS, Varadavenkatesan T, Vinayagam R, Selvaraj R. Photocatalytic zinc oxide nanoparticles synthesis using *Peltophorum pterocarpum* leaf extract and their characterization. Optik. 2019;185:248-55. doi: 10.1016/j.ijleo.2019.03.101.
23. Barzinjy AA, Azeez HH. Green synthesis and characterization of zinc oxide nanoparticles using *Eucalyptus globulus* Labill. leaf extract and zinc nitrate hexahydrate salt. SN Appl Sci. 2020;2(5):991. doi: 10.1007/s42452-020-2813-1.
24. Jayappa MD, Ramaiah CK, Kumar MAP, Suresh D, Prabhu A, Devasya RP, Sheikh S. Green synthesis of zinc oxide nanoparticles from the leaf, stem and *in vitro* grown callus of Mussaenda frondosa L.: characterization and their applications. Appl Nanosci. 2020;10:1-18. doi: 10.1007/s13204-020-01382-2, PMID 32421069.
25. Kahsay MH. Synthesis and characterization of ZnO nanoparticles using aqueous extract of *Becium grandiflorum* for antimicrobial activity and adsorption of methylene blue. Appl Water Sci. 2021;11(2):45. doi: 10.1007/s13201-021-01373-w.
26. Thattil PP, Rose AL. Enhanced removal of crystal violet dye using zinc oxide nanorods and air oxidation under sunlight radiation. Rasayan J Chem. 2020;13(2):1166-73. doi: 10.31788/RJC.2020.1325558.
27. Raliya R, Avery C, Chakrabarti S, Biswas P. Photocatalytic degradation of methyl orange dye by pristine titanium dioxide, zinc oxide, and graphene oxide nanostructures and their composites under visible light irradiation. Appl Nanosci. 2017;7(5):253-9. doi: 10.1007/s13204-017-0565-z.
28. Wang J, Chen Y, Si P, Fan R, Yang J, Pan Y, Zhao S, Shi Y. Selective fluorescence sensing and photocatalytic properties of a silver(I)-based metal-organic framework based on 9,10-anthraquinone-1,5-dicarboxylic acid and 4,4’-bipyridine ligands. Inorg Nano Met Chem. 2020;50(1):1-7. doi: 10.1080/24701556.2019.1661447.